IOPscience iopscience.iop.org

Home Search Collections Journals About Contact us My IOPscience

The buckling transition of two-dimensional elastic honeycombs: numerical simulation and Landau theory

This article has been downloaded from IOPscience. Please scroll down to see the full text article.

2004 J. Phys.: Condens. Matter 16 4419

(http://iopscience.iop.org/0953-8984/16/25/003)

View the table of contents for this issue, or go to the journal homepage for more

Download details:
IP Address: 129.252.86.83
The article was downloaded on 27/05/2010 at 15:36

Please note that terms and conditions apply.

INSTITUTE OF PHYSICS PUBLISHING JOURNAL OF PHYSICS: CONDENSED MATTER

J. Phys.: Condens. Matter **16** (2004) 4419–4428 PII: S0953-8984(04)75231-5

The buckling transition of two-dimensional elastic honeycombs: numerical simulation and Landau theory

E A Jagla

The Abdus Salam International Centre for Theoretical Physics, Strada Costiera 11, 34014 Trieste, Italy

Received 22 January 2004
Published 11 June 2004
Online at stacks.iop.org/JPhysCM/16/4419
doi:10.1088/0953-8984/16/25/003

Abstract

I study the buckling transition under compression of a two-dimensional, hexagonal, regular elastic honeycomb. Under isotropic compression, the system buckles to a configuration consisting of a unit cell containing four of the original hexagons. This buckling pattern preserves the sixfold rotational symmetry of the original lattice but is chiral, and can be described as a combination of three different elemental distortions in directions rotated by $2\pi/3$ from each other. Non-isotropic compression may induce patterns consisting of a single elemental distortion or a superposition of two of them. The numerical results compare very well with the outcome of a Landau theory of second-order phase transitions.

1. Introduction

A two-dimensional honeycomb structure formed by solid walls is the prototype of a cellular solid [1]. These are materials widely used in applications due to their remarkable mechanical properties, for instance the capacity for energy absorption under impact, and the low weight. Energy absorption is related to plastic deformation under stress. But still the ideally elastic and perfectly uniform two-dimensional honeycomb presents some not completely solved puzzles. Under compressive stress, it has a buckling transition in which some (or all) of the walls bend. This transition is reminiscent of the well known buckling transition of an elastic bar under compressive stress at its extremes [2]. There has been some controversy as regards what the buckling mode of a regular honeycomb should be. On one hand, in their original work [3], Gibson and Ashby presented the results of an experiment using an elastomeric honeycomb, under what they called biaxial loading, in which they observed a non-trivial buckling pattern consistent with a symmetry breaking in which four original cells form the new repetitive motif of the material. In a later paper [4], Hutzler and Weaire performed numerical simulations and did not observe this pattern, but instead saw a buckling mode equivalent to that obtained

 © 2004 IOP Publishing Ltd Printed in the UK

under uniaxial stress. They argue that the pattern observed in [3] was a consequence of finite size effects, and the use of flat confining walls. Numerical results taking into account these effects [5] did show the pattern observed by Gibson and Ashby. Very recently, Okomura *et al* [6] studied the problem using a combination of a homogenization technique and finite element numerical simulations. Their results do not agree with those of Hutzler and Weaire [4]. Instead, they found buckling patterns that can be interpreted as a superposition of three individual buckling modes. They also found that whether one, two, or three of these modes are active depends on the degree of anisotropy of the externally applied strain.

In view of the aforementioned contradiction between [4] and [6], and considering that the techniques employed in the two cases are quite different, an independent investigation to determine which of the two results is correct seems appropriate. In the first (numerical) part of this paper (section 2) I will show that numerical simulations done appropriately using the technique used in [4] do not support the results claimed there, but instead support those reported in [6]. In the second (more theoretical) part (section 3) I will show how the results obtained in the simulations are fully compatible with the predictions of a Landau theory of second-order phase transition applied to the buckling problem. This theory allows one to obtain at once the buckled configuration of the system under a generic form of macroscopically homogeneous applied deformation.

2. Numerical simulation

I have simulated a two-dimensional honeycomb through the technique used in [4, 5], namely by considering the honeycomb walls as one-dimensional rods, and including stretching and bending energy via

$$\begin{aligned} E_{\text{stretch}} &= \frac{1}{2}k_{\text{s}}\int\left(\frac{\mathrm{d}l}{\mathrm{d}l_0}-1\right)^2\mathrm{d}l_0 \\ E_{\text{bend}} &= \tfrac{1}{2}k_{\text{b}}\int c^2\,\mathrm{d}l_0 \end{aligned} \tag{1}$$

where c is the local curvature. To discretize these expressions I have used seven intermediate points between any two neighbour vertices, but particular cases were checked using 18 points, to guarantee the absence of noticeable effects due to discretization. The only essential parameter of the model is $k_{\text{b}}/L^2k_{\text{s}}$, where L is the length of the individual rods. This ratio is physically related to the fraction Λ of two-dimensional space that is occupied by the rods [1, 4], namely $\Lambda = 4\sqrt{k_{\text{b}}/L^2k_{\text{s}}}$. The simulations presented below were done at $k_{\text{b}}/L^2k_{\text{s}} = 4.5\times10^{-4}$ (thus $\Lambda = 0.085$), but additional checks indicate that the results are not qualitatively dependent on the precise value of the parameter. All previously obtained buckling patterns for perfect honeycombs can be accommodated within a 2×4 unit cell. Then the elemental cell that I simulated is precisely the 2×4 cell shown in figure 1(a), with periodic boundary conditions. The simulation method consists in calculating the forces acting on all points of the discretized system, and relaxing their positions using a viscous dynamics. The control variable was the macroscopic strain, which can be changed by varying the size and shape of the simulation box. Stresses in the system can be evaluated both by numerical differentiation of the total energy with respect to strain, and by direct summation in terms of the forces between particles. The equivalence of the two results allows one to check for consistency and convergence of the simulation.

Before indicating the results obtained, it is clarifying to discuss qualitatively the behaviour observed (see [6]). The buckling structures that appear are related to reaccommodation of the vertices of the honeycomb structure, in such a way that lines of vertices forming zigzag chains

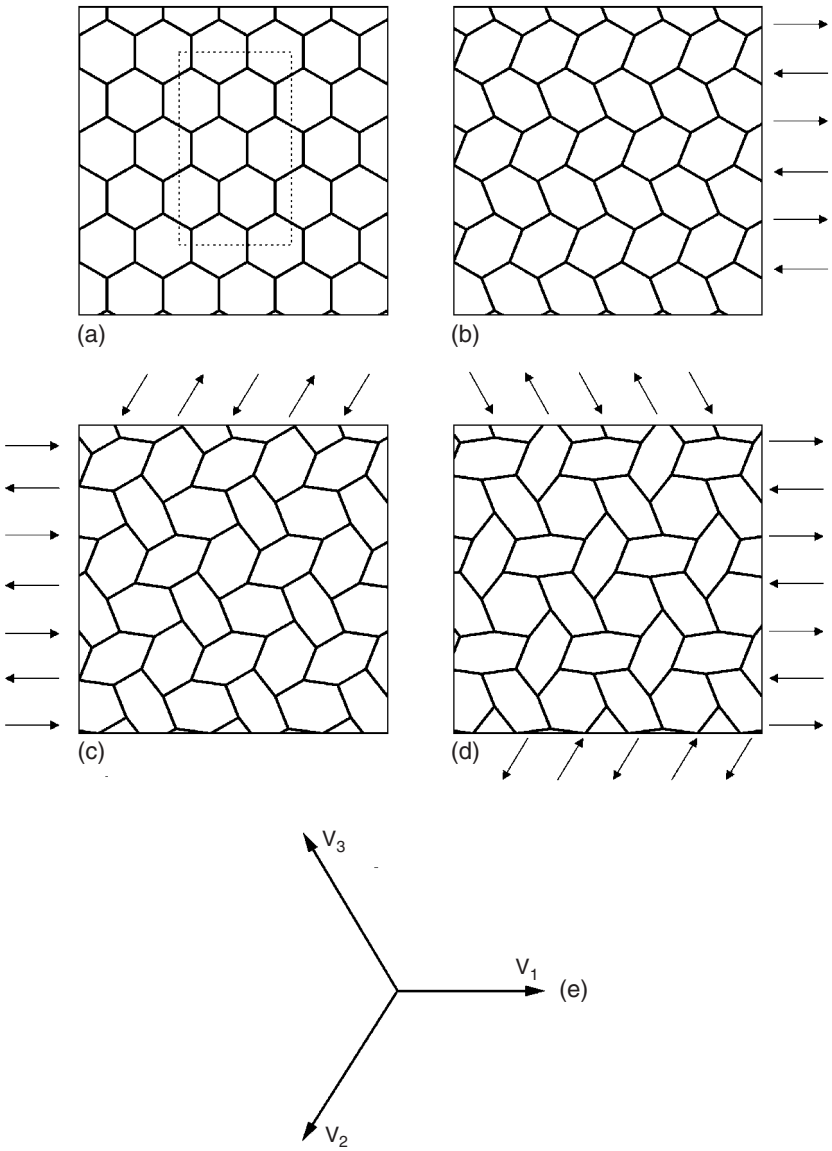

Figure 1. (a) The hexagonal starting lattice. The dotted box is the system actually simulated. (b) Upon shifts of the vertices as indicated by the arrows, the uniaxial pattern is obtained. Note however that there are three equivalent ways of generating this pattern, that can be characterized by the unitary vectors shown in (e). Combining two or the three of them we obtain the configurations in (c) and (d).

shift relatively to neighbour chains, as qualitatively indicated in figure 1(b). There are three of these modes, that will be referred to as the elementary modes of buckling. The patterns that they (individually) generate will be called the uniaxial patterns. They are characterized by the unitary vectors shown in figure 1(e). Whether one, two, or the three elementary modes acquire non-zero amplitude at the buckling transition depends on the macroscopic strain applied. The qualitative pictures of figures 1(c) and (d) show the effect of combining two or three elementary

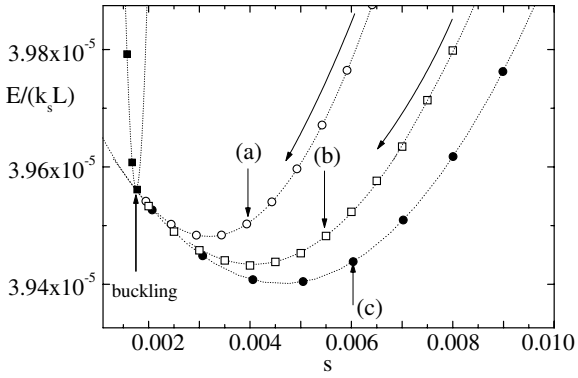

Figure 2. Total energy of the simulated system (dotted box in figure 1(a)) as a function of compressive strain $s \equiv (s_x + s_y)/2$. A global, linear contribution in s has been subtracted to allow appreciation of tiny differences in energy. All continuous lines are quadratic fittings of the data close to the buckling point. Results are shown from a run from the unbuckled state (full squares and circles), and for runs reducing strain from a large value, initializing the system in a Gibson–Ashby (open squares) or uniaxial (open circles) pattern. These two branches are actually unstable (the true minimum corresponds to the symmetric pattern), but they may last long enough for the simulations to be performed to a good accuracy (letters indicate where the snapshots in figure 3 were taken).

modes. We see that the patterns of figures 1(b) and (c) are identical (except for the wall bending, that in this qualitative picture is not taken into account) to the patterns in [3]. The pattern in figure 1(c) will be referred to as the Gibson–Ashby pattern. The pattern in figure 1(d), that combines the three elementary modes, preserves the hexagonal symmetry of the structure (this will be referred to as the symmetric pattern). A buckling mode of this symmetry has been observed and simulated in [7], but only in the case of *plastic* buckling. To my knowledge, the only prediction of this mode for a perfectly elastic honeycomb is contained in [6]. It is remarkable that this pattern has lost the mirror symmetry plane of the original structure: it is a chiral pattern. The chirality can be defined as the sign of the product of the amplitudes of the three elementary modes from which the pattern is constructed.

In the numerical simulations, I started from the unstrained structure and applied an isotropic compression $s \equiv (s_x + s_y)/2$. The system compresses uniformly until a well defined critical compression value s_c is reached. This is the buckling point of the system. For $s > s_c$ the walls of the hexagonal cells bend. In figure 2 (full symbols) we can see the results for the mechanical energy of the system in a simulation in which the uniform strain s is increased at a constant rate. At the buckling point ($s = s_c \simeq 0.00185$) the system passes from the unbuckled to the symmetric pattern (see the snapshot (c) in figure 3). Then, the numerical simulations indicate that the symmetric pattern is the stable configuration after buckling, for uniform compression. This is compatible with the results in [6].

A particularity of the simulations has to be mentioned here. Although the symmetric configuration is the lowest energy one after buckling, the uniaxial and Gibson–Ashby patterns correspond to saddles of the mechanical energy (see the Landau theory below), and they are only slightly higher in energy than the true minimum. Then, if the system is prepared in one of these configurations at large strain (in the buckled region) and a simulation is run decreasing s, the system may have no available time to run away from the saddle. In this way, simulations allow one to follow also the energy of the (unstable) branches corresponding to one, or two elementary modes active. These are shown in figure 2 with open symbols, and snapshots along these paths are shown in figures 3(a) and (b).

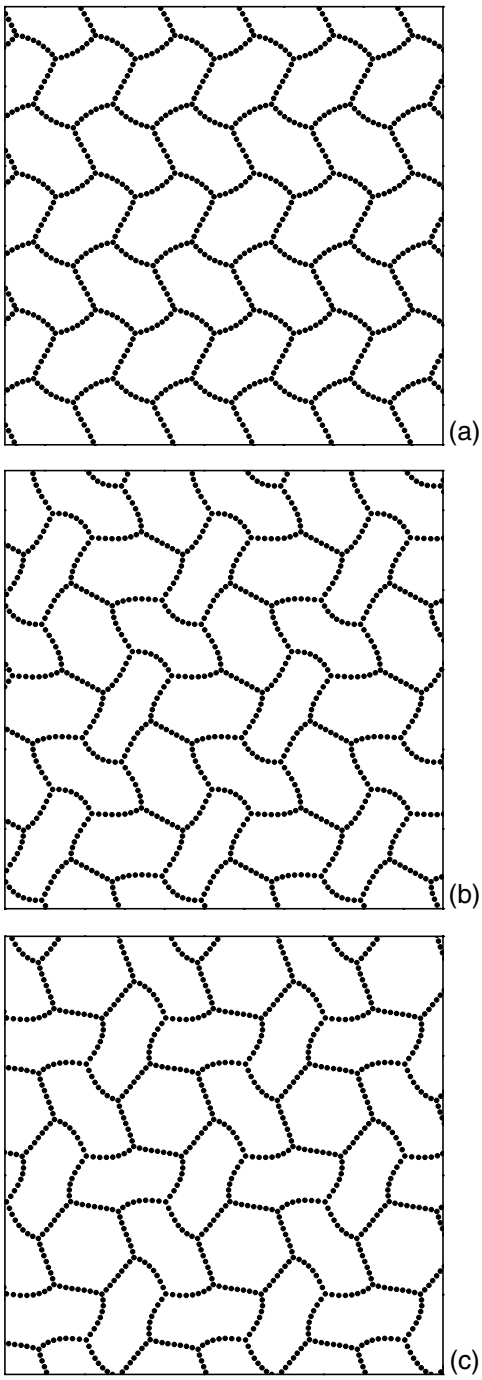

Figure 3. The uniaxial, Gibson–Ashby, and symmetric buckling modes. The snapshots correspond to the points indicated in figure 2 (the displacements with respect to the hexagonal configuration have been amplified by a factor of 5 to render the geometrical structure more visible). For isotropic compression, the symmetric pattern provides the minimum energy; the other two correspond to saddles, and eventually destabilize. However, they can be made stable under appropriate non-isotropic loading.

The uniaxial and Gibson–Ashby patterns may become the stable buckling modes under appropriate non-isotropic loading. For instance, by compressing along the x (y) direction, and keeping the perpendicular direction unstrained, I have observed the Gibson–Ashby (uniaxial) pattern to be stable after buckling. The stability of the Gibson–Ashby pattern under particular uniaxial loading agrees again with the results in [6], but not with those claimed in [4].

I can only speculate about the reasons that the correct buckling modes (for isotropic compression, for instance) were not obtained in [4]. It is possible that in the starting configuration used in [4] some tiny degree of anisotropy was present, and then the system first went to a uniaxial pattern (favoured by this anisotropy). However, this pattern is unstable, and should eventually transform to the true ground state. But the energy gain for this transformation is tiny, and the time necessary for it to occur might be much larger than the simulation time in [4], and then the true ground state would be missed.

3. Landau theory of the buckling transition

The results presented in the previous section are enough numerical input for constructing the Landau theory of this peculiar second-order transition. In fact, we see in figure 2 that the energies of all buckled configurations (whether the true minimum or the saddles) meet together in value and derivative at the buckling point, coinciding also at that point in value and derivative with the branch corresponding to the unbuckled system. This means that at the buckling point, in a generic parameter space, the state point of the system passes from a configuration with a single minimum (for the unbuckled state) to one with different minima and saddles in a continuous manner.

I will present a Landau description in which the order parameters are the three (small) amplitudes ϕ_1, ϕ_2, ϕ_3 of the elementary modes. For convenience, these three modes will be associated with the unitary vectors $\mathbf{v}^1$, $\mathbf{v}^2$, and $\mathbf{v}^3$ shown in figure 1(e). The free energy of the system (in the present case it actually corresponds simply to the elastic energy) must be a scalar, and thus it can only contain combinations of the amplitudes and the (eventually anisotropic) external strains that are invariant with respect to the symmetry operations of the lattice. Considering for the moment only the isotropically compressed case, we should look for invariant combinations of the amplitudes. Up to fourth order those available are

$$\begin{aligned} &\phi_1^2+\phi_2^2+\phi_3^2 \\ &\left(\phi_1^2+\phi_2^2+\phi_3^2\right)^2 \\ &\phi_1^2\phi_2^2+\phi_2^2\phi_3^2+\phi_3^2\phi_1^2. \end{aligned} \tag{2}$$

Then in this case the most general form of the free energy describing a second-order transition is

$$F=\alpha(s_c-s)\left(\phi_1^2+\phi_2^2+\phi_3^2\right)+\beta\left(\phi_1^2+\phi_2^2+\phi_3^2\right)^2-\gamma\left(\phi_1^2\phi_2^2+\phi_2^2\phi_3^2+\phi_3^2\phi_1^2\right) \tag{3}$$

with numerical constants α, β, and γ. This free energy has a single minimum at $\phi_p=0$ ($p=1,2,3$) for $s<s_c$, representing the unbuckled state. For $s>s_c$, this expression has saddles (or minima) at the following values of the amplitudes:

$$\phi_p^2=A \qquad \phi_q=0 \qquad \phi_r=0 \tag{4}$$

$$\phi_p^2=B \qquad \phi_q=B \qquad \phi_r=0 \tag{5}$$

$$\phi_p^2=C \qquad \phi_q=C \qquad \phi_r=C \tag{6}$$

where p, q, r are arbitrary permutations of 1, 2, 3, and A, B, C are given by

$$A=\frac{(s-s_c)\alpha}{2\beta} \tag{7}$$

$$B = \frac{(s - s_c)\alpha}{4\beta - \gamma} \tag{8}$$

$$C = \frac{(s - s_c)\alpha}{6\beta - 2\gamma}. \tag{9}$$

They correspond respectively to the uniaxial, Gibson–Ashby, and symmetric patterns. The corresponding values of the free energy are

$$f_{uni} - f_{unb} = -\frac{(s_c - s)^2\alpha^2}{4\beta} \tag{10}$$

$$f_{GA} - f_{unb} = -\frac{(s_c - s)^2\alpha^2}{4\beta - \gamma} \tag{11}$$

$$f_{sym} - f_{unb} = -\frac{(s_c - s)^2\alpha^2}{4\beta - 4\gamma/3}. \tag{12}$$

(I have subtracted the free energy of the unbuckled system f_{unb}, that is taken as zero in the Landau theory, but that should be included when comparing with the results of the numerical simulations.) We see that the symmetric pattern is the minimum energy one for $\gamma > 0$ (whereas the uniaxial pattern provides the absolute minimum if $\gamma < 0$). Then, in order to obtain agreement with the simulation results, we will assume $\gamma > 0$. The physical justification for the positive sign of γ is not provided by the Landau theory, and should come from an explicit evaluation of the mechanical energy of the honeycomb, that I will not attempt.

From the previous values of the free energy a parameter free relation can be obtained and compared with the numerical results. First note that the ratio γ/β can be obtained for instance from (10) and (12) as

$$\frac{\gamma}{\beta} = 3\left(\frac{f_{sym} - f_{uni}}{f_{sym} - f_{unb}}\right). \tag{13}$$

Using the values of energy obtained in the simulations (figure 2), we obtain approximately $\gamma/\beta \simeq 0.01$ for the parameters of the simulation. Then the second terms in the denominators of (11) and (12) are small compared to the first terms, and to a very good approximation we can obtain

$$\frac{f_{GA} - f_{sym}}{f_{uni} - f_{sym}} = \frac{1}{3}. \tag{14}$$

This is a parameter free relation that has to be satisfied in our numerical simulations. From the data in figure 2, it can be in fact verified that this is very accurately satisfied. This is a strong evidence that the present Landau theory describes correctly the physics of the buckling transition.

In order to make the theory more complete, I want to consider now the possibility of non-isotropic external loading on the system. This means that instead of a single parameter s, we have now a generic (symmetric) strain tensor s_{ij} ($i, j = 1, 2$) applied to the system (the previously introduced isotropic compression s is related to the trace of this tensor). This has to be introduced into the free energy in a symmetrically invariant form. To lowest order I will include it only in the second-order term, which is the one that triggers the transition. Two different quadratic terms in the amplitudes can be written out:

$$F^{(1)} \sim \sum_{i,j=1,2} \sum_{p,q=1,2,3} s_{jj} v_i^p v_i^q a_{pq} \phi_p \phi_q \tag{15}$$

$$F^{(2)} \sim \sum_{i,j=1,2} \sum_{p,q=1,2,3} s_{ij} v_i^p v_j^q b_{pq} \phi_p \phi_q. \tag{16}$$

Here ϕ_q is the amplitude of mode q, v_i^q is the i component of the corresponding unitary vector (figure 1(e)), and a_{pq} and b_{pq} are arbitrary numerical matrices. However, these expressions have to be invariant under symmetry operations. In particular, permutation of any two elementary vectors is obtained by a mirror symmetry along the line containing the third vector. Also, a change of sign of any of the amplitudes can be obtained by a particular spatial translation allowed by symmetry. Using these invariances, it can be obtained that both a_{pq} and b_{pq} matrices should be proportional to the identity, i.e.,

$$F^{(1)} \sim \sum_{i,j=1,2} \sum_{p=1,2,3} s_{jj} v_i^p v_i^p \phi_p^2 \tag{17}$$

$$F^{(2)} \sim \sum_{i,j=1,2} \sum_{p=1,2,3} s_{ij} v_i^p v_j^p \phi_p^2. \tag{18}$$

Then $F^{(1)}$ becomes proportional to $(\phi_1^2 + \phi_2^2 + \phi_3^2)$ and is the term considered in the isotropically compressed case.

To analyse the second contribution it can be more convenient to use the following definition of the three independent components of the strain tensor:

$$s = (s_{11} + s_{22})/2$$
$$s_2 = (s_{11} - s_{22})/2$$
$$s_3 = s_{12} = s_{21}$$

which represent the applied deformation in a more physical way: s represents an isotropic compression (we already used this), whereas s_2 and s_3 are the two independent shear modes, which are related by a $\pi/4$ rotation. In terms of these variables, and using explicitly the components of the unitary vectors, we finally arrive at the following form of the free energy:

$$F = \alpha \left[(s_c - s)\left(\phi_1^2 + \phi_2^2 + \phi_3^2\right)\right] + \delta \left[s_2 \left(\phi_1^2 - \phi_2^2/2 - \phi_3^2/2\right) + s_3 \frac{\sqrt{3}}{2} \left(\phi_3^2 - \phi_2^2\right) \right]$$
$$+ \beta \left(\phi_1^2 + \phi_2^2 + \phi_3^2\right)^2 - \gamma(\phi_1^2\phi_2^2 + \phi_2^2\phi_3^2 + \phi_3^2\phi_1^2). \tag{19}$$

This is the final expression for the free energy close to the buckling transition. Minimizing it we can obtain the buckled state under any particular combination of the three independent strains s, s_2, and s_3.

I want to describe now the buckling mode map of the system, namely, what the amplitudes of the three elementary modes are for any choice of the strain tensor. First of all note the following scaling of the free energy: if we consider the values of the three order parameters at the minimum of equation (19), namely $\phi^p_{\min}$, to be a function of $s_c - s$, s_2, and s_3, then the following relation is satisfied:

$$\phi^p_{\min}(s_c - s, s_2, s_3) = \lambda^{-1/2} \phi^p_{\min}(\lambda(s_c - s), \lambda s_2, \lambda s_3). \tag{20}$$

This implies, in particular, that the borders between different regions in the parameters space $s_c - s$, s_2, and s_3 are spanned by rays propagating from the origin.

I will analyse a couple of particular cases. First consider the case $s_3 = 0$, i.e., purely compressive strains along x and y (although not necessarily equal). I show in figure 4(a) the map of buckling modes in the s–s_2 plane for this case. The borders between different regions can be worked out analytically. All of them are straight lines emanating from the point $s = s_c$, $s_2 = 0$, as the previous argument indicates. The transition between unbuckled ($\phi_p \equiv 0$) and uniaxial pattern ($\phi_1 \neq 0$) can be easily obtained setting $\phi_2 = \phi_3 = 0$ in equation (19). The limit line is given by $s_2 = (s - s_c)\alpha/\delta$. The transition line between the unbuckled and the Gibson–Ashby patterns ($\phi_2 = \phi_3 \neq 0$) is obtained along the same lines, as $s_2 = -2(s - s_c)\alpha/\delta$.

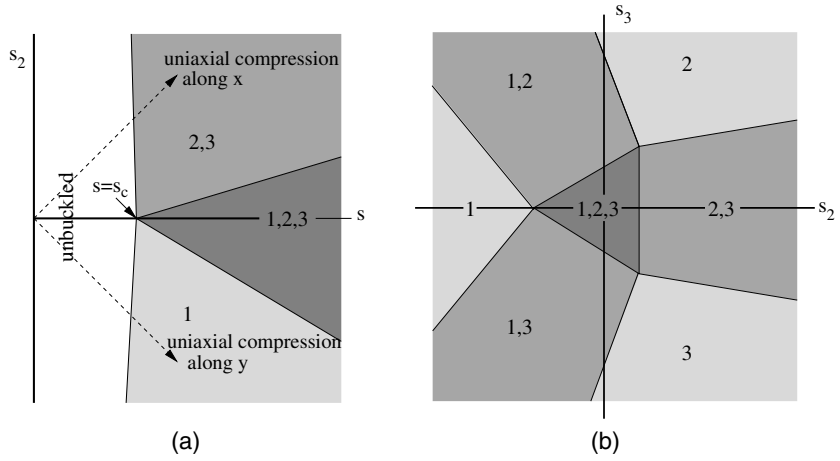

Figure 4. The buckling mode map in the s–s_2 plane for $s_3 = 0$ (a), and in the s_2–s_3 plane for a constant value of $s > s_c$ (b). In each region, the numbers indicate which elementary modes are active (see figure 1). The analytical expressions for the limits between different regions are given in the text.

Increasing s at $s_2 = 0$, the symmetric pattern appears at $s = s_c$, as we already know from the isotropically compressed case. The symmetric pattern loses its strict rotational symmetry for any $s_2 \neq 0$. However, it still has the three elementary modes active as long as we are within the darkest region in figure 4(a). The limits of this region are given by

$$s_2^{(\mathrm{uni}\to\mathrm{sym})} = -\frac{1}{3}\frac{\alpha\gamma}{\beta\delta}\frac{s - s_c}{\left(1 - \frac{\gamma}{3\beta}\right)} \tag{21}$$

for the transition to the uniaxial pattern, and

$$s_2^{(\mathrm{GA}\to\mathrm{sym})} = \frac{1}{6}\frac{\alpha\gamma}{\beta\delta}\frac{s - s_c}{\left(1 - \frac{\gamma}{3\beta}\right)} \tag{22}$$

for the transition to the Gibson–Ashby pattern. Note the exact relation

$$s_2^{(\mathrm{GA}\to\mathrm{sym})}/s_2^{(\mathrm{uni}\to\mathrm{sym})} = -2 \tag{23}$$

valid for any values of the parameters of the free energy.

The results of figure 4(a) are fully compatible with the numerical results in [6]. In particular, it can be seen that relation (23) is well satisfied in their numerical simulations. Then the present theory also explains satisfactorily the numerical results of [6]. We note that for the present parameters the stability of the uniaxial and Gibson–Ashby patterns that is obtained numerically under uniaxial compression is recovered (along dotted lines in figure 4(a)).

As an additional example I show the map of buckling modes in the s_2–s_3 plane for some $s > s_c$ in figure 4(b). Note the nice symmetry of this pattern, which has one, two, or three elementary modes active depending on the particular choice of the applied strains s_2 and s_3 (remember that s_2 and s_3 are related by a rotation of $\pi/4$). Again, all borders between different sectors are straight lines. The analytical expression for the line separating sectors 1 and 1, 3 is given by

$$s_3 = \sqrt{3}s_2\left(1 - \frac{\gamma}{3\beta}\right) - \frac{\alpha\gamma}{\sqrt{3}\beta\delta}(s_c - s). \tag{24}$$

All other lines can be obtained then from symmetry.

To finish, we note that all transitions in the parameter space are continuous, namely, there are no jumps of the order parameters at any point, and there is no possibility of metastabilities either.

4. Conclusions

The buckling mode of an elastic two-dimensional honeycomb provides an example of non-trivial patterns with symmetry breaking appearing in a very simple mechanical system. Remarkably, for isotropic compression the symmetry breaking produces the appearance of a chiral ground state. This problem is also a realization of a second-order transition that can be accurately modelled through a Landau theory constructed on the basis of the symmetry of the problem. The agreement between the Landau theory and the numerical simulation is seen to be very good.

References

[1] Gibson L J and Ashby M F 1988 *Cellular Solids: Structure and Properties* (Oxford: Pergamon)
[2] Timoshenko S P and Gear J P 1961 *Theory of Elastic Stability* (Tokyo: McGraw-Hill)
[3] Gibson L J and Ashby M F 1988 *Cellular Solids: Structure and Properties* (Oxford: Pergamon) p 99
[4] Hutzler S and Weaire D 1997 *J. Phys.: Condens. Matter* **9** L323
[5] Hutzler S and Weaire D 1999 *The Physics of Foams* (Oxford: Clarendon)
[6] Ohno N, Okumura D and Noguchi H 2002 *J. Mech. Phys. Solids* **50** 1125
Okumura D, Ohno N and Noguchi H 2002 *Int. J. Solids Struct.* **39** 3487
[7] Papka S D and Kyriakides S 1999 *Int. J. Solids Struct.* **36** 4367
Papka S D and Kyriakides S 1999 *Int. J. Solids Struct.* **36** 4397